




## Simulation of the entanglement of a North Atlantic right whale (*Eubalaena glacialis*) with fixed fishing gear

**LAURENS E. HOWLE**,<sup>1</sup>  Department of Mechanical Engineering and Materials Science, Duke University, Durham, North Carolina 27708, U.S.A. and Department of Radiology, Duke University Medical Center, Durham, North Carolina, 27710, U.S.A.; **SCOTT D. KRAUS**, Anderson Cabot Center for Marine Life, New England Aquarium, Boston, Massachusetts 02110, U.S.A.; **TIMOTHY B. WERNER**, Anderson Cabot Center for Marine Life, New England Aquarium, Boston, Massachusetts 02110, U.S.A. and Department of Biology, Boston University, 5 Cummington Mall, Boston, Massachusetts 02215, U.S.A.; **DOUGLAS P. NOWACEK**, Nicholas School of the Environment and Pratt School of Engineering, Duke University Marine Laboratory, Beaufort, North Carolina 28516, U.S.A.

### ABSTRACT

Population estimates of the critically endangered North Atlantic right whale (*Eubalaena glacialis*) put the number of individuals at 458 with the actual number likely being lower due to a recent unusual mortality event. Entanglement with fixed fishing gear is the most significant cause of mortality of North Atlantic right whales. There remains little documentation of how North Atlantic right whales become enwrapped during an encounter with fixed fishing gear. In order to gain a better understanding of how entanglements might occur, an interactive simulator was developed that allows the user to swim a virtual whale model using a standard game controller through a gear field in an attempt to re-create an entanglement. The morphologically accurate right whale model produces realistic swimming motions and is capable of pectoral fin motions in response to user input. Using the simulator, gear entanglements involving the pectoral flippers including ropes wrapping around the body and entanglements involving the tailstock were re-created. Entanglements involving the pectoral flippers with body wraps were more easily generated than entanglements involving the tailstock only. The simulator should aid scientists, fisheries experts, fishing gear designers, and bycatch reduction scientists in understanding entanglement dynamics and testing potential new gear configurations.

Key words: North Atlantic right whale, *Eubalaena glacialis*, wildlife management, entanglement, fishing gear, simulation.

<sup>1</sup>Corresponding author (e-mail: laurens.howle@duke.edu).

The North Atlantic right whale (*Eubalaena glacialis*) has been fully protected from commercial hunting since 1935, but the species is still listed under the U.S. Endangered Species Act and as critically endangered on the International Union for the Conservation of Nature and Natural Resources (IUCN) Red List (<http://www.iucnredlist.org>). Further, the species is protected under both the U.S. Marine Mammal Protection Act and the Canadian Species at Risk Act, which prohibit “takes.” The only known population of this species, which mainly occurs in coastal waters from Florida to eastern Canada, has shown a recent decline with a population estimate of 458 individuals including 272 males and 186 females (Pace *et al.* 2017). In 2017 there was an Unusual Mortality Event, primarily in Canada, resulting in 17 confirmed stranded whales with an additional five live whale entanglements (NOAA Fisheries 2018) indicating that the number of NARWs is likely lower than 458. To address the injury and mortality from ship strikes, several measures have been taken such as shifting shipping lanes in the United States and Canada and the recent implementation of a speed reduction rule around ports along the U.S. East Coast (U.S. Federal Register 2013); these measures appear to have successfully reduced ship strikes (Laist *et al.* 2014). However, mandated changes to fixed fishing gear, especially targeting lobster pot “trawls,” have not resulted in a reduction in the entanglement rates of NARWs and other species (Pace *et al.* 2014). Recent changes by the Canadian Government to reduce right whale mortality include earlier snow crab gear removal, prohibited fishing in right whale foraging habitats, dynamic closures when whales are found, increased snow crab licensing and reporting requirements, required reporting of all commercial interactions with marine mammals, increased aerial and on-water surveillance for right whales in the Gulf of St. Lawrence; among others.

### *Mortality from Entanglement*

Becoming entangled in fishing gear is dangerous for whales for several reasons. Direct mortality from gear has been documented, but more common is the gradual decrease in body condition associated with gear being wrapped around body parts, including the mouth, reducing the animal’s ability to feed (Pettis *et al.* 2004, Johnson *et al.* 2005, Moore *et al.* 2006, Cassoff *et al.* 2011, Moore and van der Hoop 2012, Barratclough *et al.* 2014). Even when not involving the mouth, entanglements force animals to expend additional energy as they drag gear through the water (van der Hoop *et al.* 2014) and have been shown to reduce survival (Robbins *et al.* 2015). A recent retrospective study using photographic evidence (*i.e.*, scars) of current or past entanglements found that of 626 individual whales assessed over a 30 yr time period (1980–2009), 82.9% had evidence of at least one entanglement and 59% of those animals had been entangled more than once (Knowlton *et al.* 2012). Repeat entanglements are dangerous as the odds of an entanglement leading to a serious injury or mortality increases. Annual rates of serious entanglement (*e.g.*, causing life-threatening wounds) in the population have been as high as 3% and average *ca.* 1.5% over the 30 yr period. Also of

concern, is the annual rate of all entanglements, which, for the 30 yr period averaged 25.9%. *Inter alia*, this annual entanglement rate indicates that many entanglements go undetected and that some whales do manage to free themselves from gear.

### *Regulatory Changes to Reduce Entanglement*

In an attempt to reduce entanglements in U.S. waters, the National Marine Fisheries Service (NMFS) has implemented several regulations mandating modifications to gill net and pot gear in the eastern United States, including prohibition on the use of floating line at the surface, time-area closures, the use of weak links in buoy lines and net panels, a requirement that lines joining fishing traps along the sea bottom must be negatively buoyant (*i.e.*, so-called “floating” line is believed to entangle whales as they swim close to the bottom to feed) (Brillant and Trippel 2010), and reducing the ratio of vertical lines/lobster pots (“trawling up”) (see <https://www.greateratlantic.fisheries.noaa.gov/protected/whaletrp/plan/index.html> for a full list of regulatory requirements). There remains a threat in the water associated with traps and gill nets as the ropes connecting bottom gear to surface buoys (hereafter referred to as “buoy lines”) number in the hundreds of thousands (Myers *et al.* 2007), and in some near-shore areas of Maine trap fishermen are exempted from using sinking groundlines under the Atlantic Large Whale Take Reduction Plan. Another means of addressing the entanglement problem is to remove the gear from an entangled swimming whale, an operation that is expensive and dangerous for both whales and humans. Even with the successful removal of gear, animals can carry life-long injuries (Johnson *et al.* 2005, Cassoff *et al.* 2011, Barratclough *et al.* 2014), with consequences that can be fatal, even if the whale is completely disentangled (Moore *et al.* 2006, Moore and van der Hoop 2012, van der Hoop *et al.* 2017). Also, while disentanglement is sometimes successful, many more animals become entangled than can be helped and many entanglements are known through the existence of scars from previous entanglement events (Knowlton *et al.* 2012).

### *Whale Vision*

To reduce the probability of right whale entanglements in fishing gear, scientists and gear developers have considered the feasibility of visually enhancing ropes and nets to improve their detectability by whales. Studies on right whales in Cape Cod Bay using buoy line mimics, constructed from painted PVC pipe, suggest that changing buoy line color could improve the ability of right whales to reduce line encounters during daylight hours (Kraus and Hagbloom 2016). Whales were able to detect red and orange at the farthest distances (averages 3.85 m and 4.1 m), black at an intermediate distance (3.1 m average), and green at the closest distance (1.9 m average). These trials also showed that right whales will make drastic maneuvers to avoid collisions when they see ropes in their path but did not always do so. Red and orange ropes are likely to improve the distance of detection to a point where whales have enough warning to successfully avoid ropes. At the very least, eliminating green and white ropes from fixed gear is

likely to reduce collision probabilities in all fisheries that encounter right whales (Kraus and Hagbloom 2016).

The method we have taken to contribute to this search for solutions is to re-create the sequence of whale behavior that can lead to entanglements and to “reverse engineer” the situation in order to provide an accurate tool to assess the effect of proposed gear changes. Here, reverse engineering is defined as beginning with photographs or drawings of an entangled whale and attempting to re-create the whale behavior at first encounter with the fixed fishing gear that resulted in that particular entanglement. A virtual whale entanglement simulator (VWES) was created to do this, and the simulation environment also returns information on the forces (friction, drag, gear force on whale, rope tension) experienced by the whale and the gear during an encounter. We discuss here the VWES and report our experience in re-creating the entanglements of Eg 3445 and Eg 3107.

In addition to providing a tool that marine mammal scientists can use to reverse engineer whale entanglement events, an additional motivation for this work was to create a virtual gear design software system in which fishing gear designers and marine fisheries regulators can test gear modifications virtually. In general, evaluating modified gear is too difficult to test in the field, including in actual fisheries, because the studies may be overly expensive, time-consuming, or pose too much risk to whales. The VWES can potentially provide a platform to help gear designers and regulators develop and promote gear types that reduce the probability and/or severity of whale entanglements. The VWES was developed as a *serious game* (Iuppa and Borst 2010) that allows the researcher to directly control the whale’s movement in real time through the use of a game-style controller and test various whale behavior and gear interaction scenarios.

## METHODS

### *Render Engine*

Several application programming interfaces (APIs) were investigated for displaying the graphical output from the VWES system. Two of the more popular graphics APIs are OpenGL and Direct3D (Miller *et al.* 2009). Direct3D was developed by the Microsoft Corporation and is a proprietary API for use with the Windows operating system. OpenGL was originally created by the Silicon Graphics Corporation and has become a widely used open-standard API. Both of these graphics APIs will take advantage of hardware acceleration if the capability exists on the computer’s graphics card (Miller *et al.* 2009). A third graphics API set, XNA, is a proprietary Microsoft system that provides a managed wrapper for the Direct3D and DirectX API sets (Cawood and McGee 2009, Harbour 2010, 2012; Jaegers 2010; Miller and Johnson 2011; Miles 2011; Reed 2011). After a review of the competing technologies, the XNA 4.0 Game Studio programming API was selected. An advantage of developing under the XNA API is that the modeling system can be deployed to either computers running Microsoft operating systems or to

Xbox game consoles. Although now deprecated by the Microsoft Corporation, XNA is an API frequently used to program Xbox and many Windows games. This API set offers many advantages to the programmer when developing graphics-intensive applications such as native integration with the managed C# computer programming language.

### *Physics Engine and Calculations*

The dynamic behavior of the gear and collision detection turned out to be two of the major areas of effort for this project. In order to automate many of these calculations, a commercial, off-the-shelf (COTS) physics engine (DigitalRune 2014) that includes dynamic physics models, collision detection, and many other physics simulation capabilities was selected. While other physics engine systems are available (Emperore and Sherry 2015), the COTS physics engine API that was particularly well-suited to this project due to its low cost, relative ease of programming, and ease of customization.

For the entanglement reverse engineering studies considered in this paper, a typical “in-shore” trap configuration for the Gulf of Maine was used (McCarron and Tetreault 2012). While there are many variants of this gear type, it was decided to use a single 18 kg, 0.91 m × 0.61 m × 0.36 m lobster trap with a 1.27 cm diameter becket connecting to a 1.27 cm diameter floating buoy line portion spliced to a 1.27 cm diameter sinking buoy line portion with an overall scope of 2:1 (see Fig. S1). While the entanglement case studies considered in this paper had smaller rope diameters (for example, 0.95 cm) it was found that the use of small diameter ropes in the VWES caused numerical issues such as numerical instability and tunneling (rope passing through the body of the whale). The surface marker consisted of a single 15 cm diameter poly ball. The simulation environment consisted of a 18 m deep water column with nearly slack tidal current and no wave action. The hydrodynamic drag on the trap was calculated for the gear drag experiments as

$$F_D = \frac{1}{2} \rho U^2 C_D A \quad (1)$$

where  $\rho$ ,  $U$ , and  $A$  are the respective fluid density, relative flow speed between the trap and the water, and the projected frontal area of the trap. For the drag coefficient,  $C_D$ , the value 1.44 was used. This drag coefficient was within the range of 0.69 (van der Hoop *et al.* 2016) and 2.3 (Budiman *et al.* 2004) for traps of similar size.

In programming the animation for the whale’s swimming motion, we wanted to make sure our system would not only look natural but also that the tail-beat amplitudes and frequencies were accurate. We expect that correct tail motions are important in trying to re-create or understand entanglements involving the peduncle and tail flukes. The swimming motion of fish (Eloy 2012) and cetaceans (Rohr and Fish 2004) has been extensively reported in the literature. Rohr and Fish (2004), when studying swimming kinematics of seven odontocete species (*Delphinapterus leucas*, *Globicephala melaena*, *Lagenorhynchus obliquidens*,

Table 1. Whale swimming movements reproducible in the current version of VWES.

Movement	Manual control	Programmable for automated model runs
Tail fluke swimming motion	X	X
Pectoral fins: forward-back sweep	X	X
Pectoral fins: tilt angle	X	X
Body roll	X	X
Ascend/descend	X	
Turn left/right	X	
Surface active group motions	X	

*Orcinus orca*, *Pseudorca crassidens*, *Stenella frontalis*, *Tursiops truncatus*) showed that peak-to-peak fluke amplitude falls in the range of 0.15–0.25 when normalized by body length. The tail-beat frequency fell in the range from 1 to 2 when normalized by the ratio of swimming speed to body length. The Strouhal number is frequently used to describe swimming kinematics and is defined by

$$St = \frac{fA}{U} \quad (2)$$

where  $f$  is the tail-beat frequency,  $A$  is the peak-to-peak tail motion amplitude (the peak-to-trough vertical excursion of the tail trailing edge), and  $U$  relative speed between the animal and the fluid. The Strouhal number in swimming animals falls within the narrow range of 0.2–0.4 with peak efficiency typically found near 0.3 (Taylor *et al.* 2003, Rohr and Fish 2004, Eloy 2012). In the VWES, as the whale's swimming speed changes, the animation controller is used to modify the frequency of the basic swimming animation so that the Strouhal number remains constant at 0.3. While the Strouhal number might increase for slower, less efficient swimming speeds, the VWES does not currently implement this effect. Due to limitations imposed by numerical instability in the rope simulations, the whale swimming speed is currently limited to a maximum of 2 m/s. The relationship between tail-beat frequency, amplitude, and swimming speed is important for re-creating entanglements involving the tailstock. Numerous body and appendage movements are programmed to test various scenarios as described in Table 1.

Fast and accurate simulation of rope dynamics with time-varying loads and time-varying contacts is an active area of current research focus, particularly in the fields of offshore structures (Flory *et al.* 2005, Lee *et al.* 2005, Tsukrov *et al.* 2005, Tahar and Kim 2008), and computer graphics (Imanishi *et al.* 2009, Servin *et al.* 2011). Information on the properties of ropes such as strength, bending stiffness, elongation, friction, and wear due to internal and external damage is extensive for fiber ropes (McKenna *et al.* 2004, Tsukrov *et al.* 2005, Tahar and Kim 2008) and

wire ropes (Costello 1997, Imrak and Erdonmez 2010). Some of the issues that arise in generating an accurate rope model for interaction with other objects include the need to balance computational speed, accuracy, and numerical stability. Rope models can be classified into two categories: continuum models and models that approximate the rope as a chain of rigid bodies (Servin *et al.* 2011). The secondary category is used in the VWES; approximating the continuous rope as either spheres or capsule shapes, which were connected to one another with virtual springs. The springs allow the force to be transmitted from one link component to the next and allowed for expedient collision detection calculations. However, if the spring constant was too large, the dynamic rope response became numerically unstable.

Solutions for the static shape of a rope under the combined effects of buoyancy, current, and tension loads due to buoys are well-known and readily available (Fridman 2008). These model solutions were used in the VWES for specifying the initial rope shape for some of the simulations. In addition, specifying a simpler initial shape allowed the rope to settle to a steady-state configuration under the combined effects of current, buoyancy, and possible contact with other objects such as traps was a benefit to the simulation. Measurements of floating ground line elevation are also available (Brillant and Trippel 2010), however, this was not implemented in the VWES because floating ground lines are decreasingly used in U.S. pot fisheries. The capacity for multipart ropes was included and allowed modeling the dynamics of a combined floating/sinking buoy line as is currently used in lobster fisheries in the northeast United States (McCarron and Tetreault 2012).

The hydrodynamic drag on a length of rope is dependent upon the rope's length and diameter, the fluid density, the angle of flow with respect to the longitudinal axis of the rope, and is proportional to the square of the flow speed. Equation 1 was used for calculating this drag force where the area was calculated as the product of the rope segment length  $L$  and diameter  $D$ . Measurements of the angle-dependent drag coefficient for 16 mm diameter steel wire rope are available (Fridman 2008). Using the data from Fridman (table 3.3, p. 64), the angle-dependent drag coefficient was applied to an even-symmetric cosine function:

$$C_D(\alpha) = 0.688 + 0.544\cos(2\alpha + \pi) \quad (3)$$

where  $\alpha = 0$  for flow aligned with the longitudinal axis of the rope segment and  $\alpha = \pi/2$  for flow perpendicular to the rope's longitudinal axis. Equation 3 was used for calculating the drag coefficient on each rope segment.

Collision detection is used to test whether or not a component, in this case a segment of rope, contacts the whale. Collision detection was determined by a common technique in computer game development (Ericson 2004), by attaching a set of convex collision primitives (spheres, boxes, cylinders, cones, capsules) to each skeleton rig bone. Then, each bone's collision primitive set was used to create a convex hull that encapsulates all of the skin vertex points for that collision

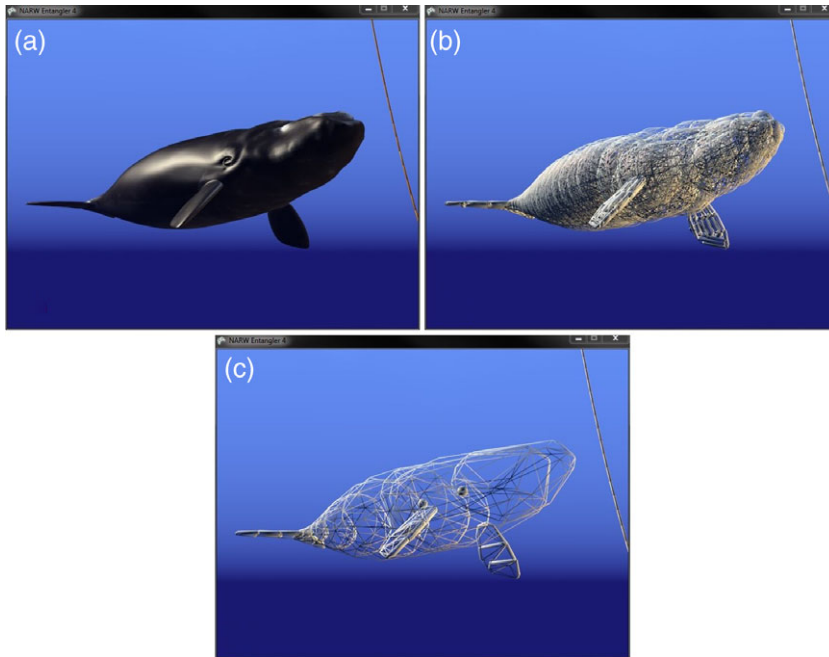


*Figure 1.* (a) shows the NARW skin mesh in proximity to a buoy line. (b) shows the complete collision set constructed from a collection of convex rigid bodies (spheres, cones, cylinders, capsules, and rectangular boxes). (c) shows individual convex hulls enclosing the collision set for each skeleton rig bone. These convex hulls, which move with their associated rig bone, are used for whale-environment collision testing and interaction.

primitive set as demonstrated in Figure 1. When the position of the whale is updated in world space or when the skeleton rig is manipulated, the bone transforms are used to update the position of the convex hulls so that they move with and articulate with the whale. Only the convex hulls are used in collision testing as this is far more computationally expedient than using either the surface mesh or the collision primitive set. If a collision is detected, then the physics engine places equal and opposite forces on both the whale and the contacting object causing the object (and/or the whale) to move. This prevents the contacting object from penetrating the whale's surface mesh.

### *Whale Model Animation and Movements*

The model of the 10 m (overall length) NARW used in the VWES model was created in several steps. First, a gaming programmer created an initial wire mesh whale using the LightWave 3D software system, basing the shapes and dimensions of the whale parts on pictures and video. The model was then imported into the Blender software package, where it was substantially revised using empirical measurements obtained from



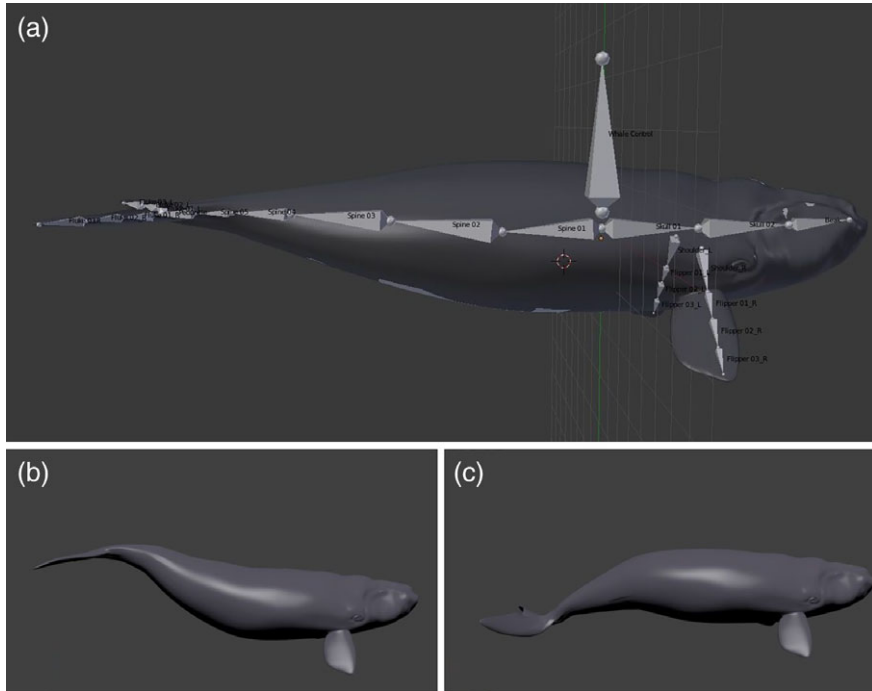


*Figure 2.* (a) shows the 10 m NARW whale model skeleton rig used for pregenerated animations and user-generated movements. The surface mesh deforms in response to movements of the skeleton rig. The vertical bone (the root bone) is used to place the whale model in world space and does not otherwise participate in animations or motions. (b) shows the whale near the top of the upstroke while (c) shows the whale near the bottom of the downstroke.

necropsy reports and from photogrammetry efforts (for full details see Nousek-McGregor 2010).

In order to animate the NARW model, standard computer graphics techniques were employed (Lever 2001) and the Blender software package to create the skeleton rig shown in Figure 2a. Each skin mesh vertex of the whale model is assigned to move in response to up to four skeleton rig bones according to an assigned mathematical weight. The surface mesh deforms in response to either preprogrammed or user-directed movements of the skeleton rig (see Table 1). Using Blender, two animations were created. The first animation is the basic bind (resting) pose for coasting whale posture, while the second animation is the basic swimming movement. The swimming animation near the top of the upstroke is shown in Figure 2b and near the bottom of the downstroke in Figure 2c. These two basic animations are imported into the VWES at load-time and the animation controller is used to smoothly map from one animation (bind or swimming) to the other. The animation controller is also used to control the speed (frequency) of the swimming

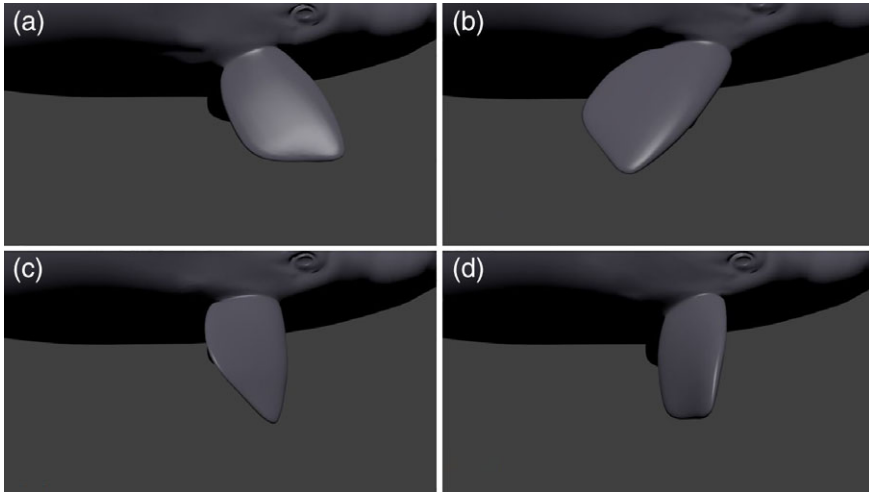


*Figure 3.* Images showing a range of flipper motions, including: (a) abduction, (b) adduction, (c) pronation, (d) supination. While cruising, many cetaceans maintain a rearward swept posture with their flippers, as shown in (b), in order to reduce drag forces. For maneuvering, the flippers are typically swept forward as (a) shows. (c) and (b) show the flippers pitched in order to produce net pitch and/or roll moments on the whale for maneuvering.

animation. In addition to these programmed animations, the user may directly control the spine and flippers by use of the game controller in order to mimic thrashing or surface-active group (SAG) motions (Table 1).

The skeleton rig, through user-input commands from the game controller, also moves and positions the pectoral flippers. For example, if the user directs the whale to surface or dive, the pitch of the whale's pectoral flippers changes relative to the whale's root bone. Flow over the pitched flippers creates a net pitching moment on the whale and causes the whale to surface or dive accordingly. If the user directs the whale to turn, the whale's pectoral flippers pitch in opposite directions and create a net rolling moment on the whale. Figure 3 demonstrates the pectoral flippers near the extremes of their range of motion.

### *Entanglement Case Studies*

A typical entanglement involving a mid-body wrap (PCCS WR-2005-18, NMFS E25-05) is shown in the aerial photograph of entangled NARW Eg 3445 in Figures 4 (upper) and 5 (upper). This whale, a 2-yr-old female born in 2004, was first observed entangled on 3 December 2005 and was partially disentangled on 12 December 2005. The gear removed from the whale included approximately 122 m of 0.95 cm and 0.79 cm poly rope with a number of splices, gangion lines, and three 20 cm yellow trawl cans. Also removed from Eg 3445 were 18.9 m of additional poly rope with a single 15 cm spherical float that was thought



*Figure 4.* North Atlantic right whales Eg 3445 (upper image) showing fishing gear wrapped around the whale's body and Eg 3107 (lower image) showing an entanglement involving the tailstock. Eg 3445 was a 2-yr-old female born in 2004, entangled 5–296 d when partially disentangled on 12 December, 2006. Eg 3107 was a 1-yr-old female with one prior entanglement interaction and was entangled 57 to 266 d when disentangled on 1 September 2002. Eg 3107 was sighted dead on 13 October 2002. Eg 3445 was last sighted in 2006 and is presumed dead. (Photo credits upper: 3 December 2005, Wildlife Trust, GA; lower: 6 July 2001, Brier Island Whale and Seabird Cruises).

to be from a separate entanglement. Based on the dates of the last entanglement-free sighting and the first entangled sighting, Eg 3445 had been entangled between 9 d and 296 d. The whale was last sighted in 2006 and is now presumed dead.

A second typical entanglement type involves wraps around the caudal peduncle and/or flukes (PDDC WR-2002-12, NNFS E15-02, accessible at <http://www.bycatch.org>), as shown in the photograph in Figure 4 (lower) with a diagram of the entangling gear shown in Figure 5 (lower). NARW Eg 3107 was a 1-yr-old female that had been entangled between 57 d and 266 d when it was first sighted entangled on 6 July, 2002. The lobster trap gear consisted of 0.95 cm polysteel/PET buoy line with one small rigid buoy and two buoy sticks. The thin line wrapped once around the caudal peduncle, twisted tightly back upon itself, and had cut deeply into the tailstock. Eg 3107 was disentangled on 1 September 2002 and confirmed dead on 13 October 2002.

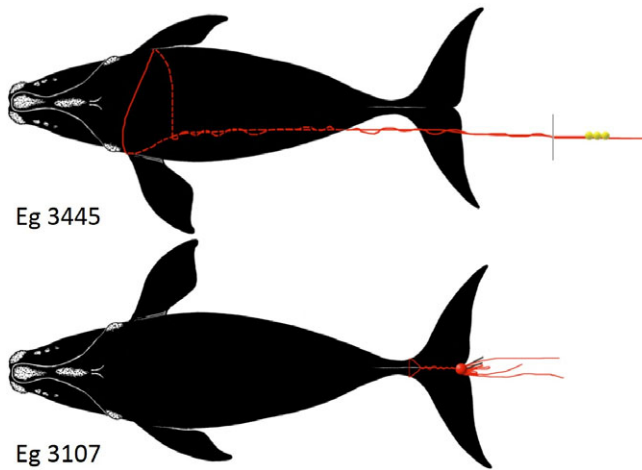


*Figure 5.* The drawing of Eg 3445 (upper) shows an entanglement (NMFS E25-05) involving a body wrap with gear consisting of 1.11 cm and 0.79 cm polysteel and 0.95 cm polypropylene buoy lines. The gear trailed 122 m behind the whale and attached to three hard buoys. The gear was from two different samples with the second sample likely caught by the first. The drawing of Eg 3107 (lower) shows a typical fluke/peduncle entanglement (NMFS E15-02). The 0.95 cm diameter line was deeply embedded in the tailstock, tightly tangled on itself, and was attached to one hard buoy and two buoy sticks. (Illustrations by S. Landry, PCCS; full case studies available at <http://www.bycatch.org>).

A third common entanglement in baleen whales involves trap rope passing through the mouth (Cassoff *et al.* 2011). For this type of entanglement, the trap line often gets wedged tightly in the baleen plates and can be difficult or impossible to fully remove. Mouth wraps also frequently additionally involve combinations of flipper and or fluke wraps. The VEWS whale model does not currently have the capability to simulate oral entanglements.

#### RESULTS AND DISCUSSION

The first case study is an entanglement involving a body wrap in the vicinity of the pectoral flippers, similar to the entanglement of Eg 3445 as shown in Figure 4 (upper) and Figure 5 (upper). The sequence of events leading to a flipper-involved body wrap is shown in Figure 6. This type of entanglement is most easily generated by having the whale initiate a rolling behavior, beginning when the buoy line is initially detected on the head by the forward-moving whale. Entanglements involving the pectoral flipper(s) are the most easily generated entanglement type using the VWES. Several factors influence whether a particular encounter would result in entanglement including flipper sweep angle, roll direction, roll rate, current speed and direction relative to the whale's path, the whale's vertical position in the water column, and gear lateral offset. Through repeated simulations, the VEWS found that

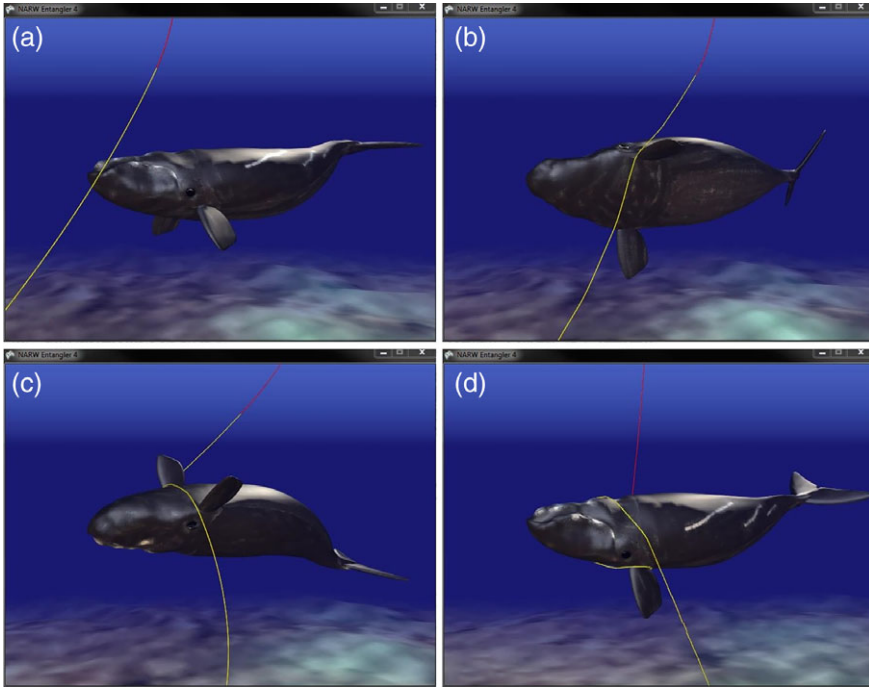


*Figure 6.* NARW becoming entangled in lobster trap gear resulting in a flipper and body wrap. This type of entanglement is most easily generated if the whale executes a roll just before encountering the buoy line. (a) shows the whale at the moment of detection while (b) shows the whale beginning the execution of a roll away from the buoy line. Note that while maneuvering the whale would likely have its flippers in the forward swept orientation. (c) shows the whale halfway through the roll which is nearly completed in (d). In our simulations, we find that if the line becomes stuck at the forward insertion of the flipper, a roll typically results in the line wrapping around the body.

flipper wraps were more difficult to generate if the flipper is maintained in the aft-swept cruising configuration (Fig. 3b). Roll direction was also an important factor on whether an encounter resulted in an entanglement. For example, if the whale detected a rope with any lateral offset (left or right of the direction of travel), and the whale rolled away from the rope the VWES found that an entanglement was more likely to result. This was because the pectoral flippers are located toward the ventral side of the centerline. Through repeated simulations of first encounter, the VWES found that for a rolling maneuver without a change in water column height, entanglements were more likely to occur for encounters near the sea floor than for encounters near the sea surface. Another important variable on whether an encounter resulted in a persistent entanglement appears to be lateral gear offset from the axis of travel. If the buoy line encounters the flipper's leading-edge closer to the tip than the root, then the flippers natural leading-edge curvature

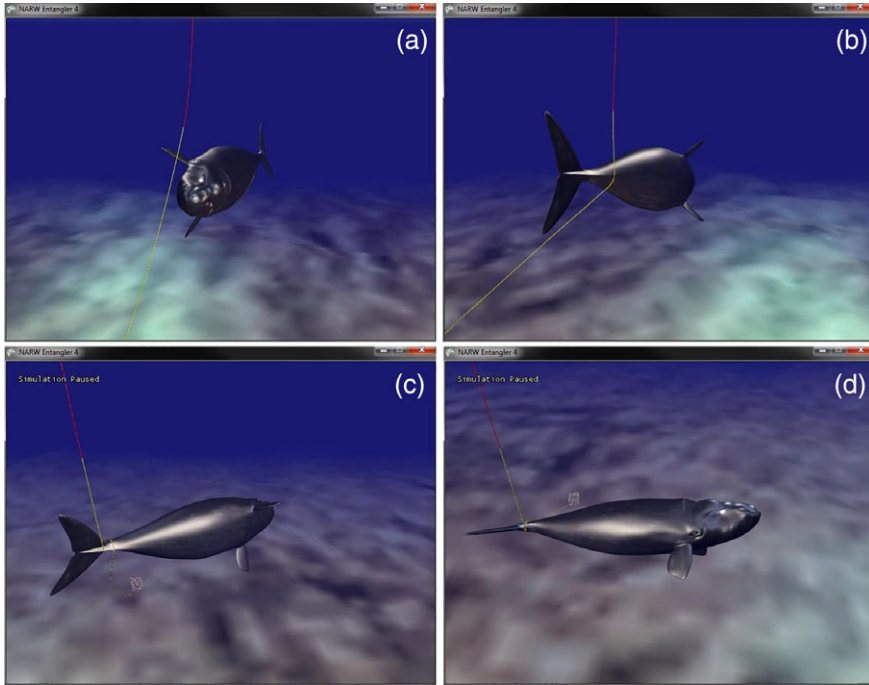


*Figure 7.* A gear encounter resulting in a peduncle wrap. We found that peduncle wraps can be generated easily by two methods. First, by turning away from (a) but interacting with (b) the rope. Subsequent lateral motions of the tailstock then result in complete wraps around the peduncle as shown in (c) and (d). The second method of generating a peduncle wrap is for the rope to wrap from one side of the peduncle over or under the flukes and trail aft. Then, a roll causes the rope to wind upon itself completing the entanglement.

was more likely to cause the rope to shed. When a flipper-involved entanglement also had one or more body wraps, friction between the rope and skin prevented the rope from sliding and resulted in a lasting entanglement.

The second case study investigated how entanglements involving the tailstock could be generated (Fig. 7). We found three possible mechanisms for entanglements initiated with the tail stock. The first mechanism was a turn to avoid the gear followed by contact between the tailstock and gear. The second mechanism was possible contact with the gear followed by surface active group motions (flailing, thrashing). The final mechanism was an encounter that initially began as a flipper or body wrap. Then, as entrained gear trailed aft, it became wrapped on the tailstock. This was followed by the rope being freed from the flipper with only the tailstock wrap remaining. This type of entanglement was most easily created by having the whale execute a combination of pitch and roll in an attempt to avoid a buoy line. The VWES found that tailstock entanglements were difficult to generate without the whale executing turning and/or surfacing behaviors.

The NARW entanglement simulation model re-created rope configurations similar to those observed from actual entanglement case studies by manipulating whale behaviors when colliding with, and in response to, buoy lines, the initial point of contact, orientation of body parts such as pectoral fins, and initial body movements by the whale in response to contacting the line. The body rolling behavior observed on two occasions for humpback whales becoming entangled in vertical ropes appeared to be a critical whale response behavior that would increase the likelihood of an entanglement. Interestingly, the possibly instinctual reaction of rolling away from the rope was shown to increase the probability that the whale would become entangled. Simulations suggest that if contact occurs deeper in the water column, keeping all other variables constant, entanglement is more likely to occur, although this will be dependent on water depth and the distance of rope from the point of contact to the water surface relative to the size of the whale and speed of roll, because a slower roll may allow for more line to shed before getting hung up on the whale. Showing how the types of real-world entanglements can occur provides a starting point for examining possible gear modifications to prevent entanglements that will be the focus of the next phase of tests using the model, and below we discuss a number of these that we will consider.

Similar to experiments using a towed NARW flipper model (Baldwin *et al.* 2009), the VWES simulations revealed that the buoy rope was more frequently shed when the flipper was swept rearward. With the flipper swept forward, the VWES did not show the rope being shed from the flipper. For encounters near the middle and especially the lower water column heights, our VWES simulations did not show the rope sliding until the buoy was in contact with the flipper. This was likely due to the imbalance in rope tension between the ascending and descending portions of the buoy like not being great enough to overcome the friction forces between the whale skin and rope. Instead, there was typically sliding until the slack was removed from both the ascending and descending portions of the rope, at which point the tension on the ascending and descending rope segments, together with the friction force of the rope on the flipper's leading edge, were balanced and the gear became entrained. For these middle and lower water column interactions, we found that the encounter was more likely to result in a lasting entanglement. Furthermore, in our study we also observed that higher tension was a factor that facilitated entanglement. Although the body of evidence to date does not indicate that increasing line stiffness is a priority for preventing whale entanglements and may even result in more severe injuries if applied, future model scenarios using the VWES can help us improve our understanding about this potential modification.

With our VWES simulations, we found that tailstock entanglements were easily generated if the whale displayed SAG-type movements after encountering the gear, and the role of this thrashing behavior in producing entanglements warrants further examination using the model.

The fisheries in which such ropes might be practically used is currently the focus of a separate New England Aquarium (Boston, MA) study with fishermen in New England, and the VWES model can serve

as a platform for further testing this hypothesis using multiple simulations of ropes with different breaking strengths.

### *Conclusion*

This study focused on modifying buoy lines in commercial fishing gear, although another alternative fishing strategy avoids the deployment of vertical ropes; and in some cases horizontal groundlines altogether. In southeastern Australia, at least two commercial lobster pot fishermen have incorporated the use of acoustically released buoy lines that remain within a mesh bag on a line that is suspended on average 18 m above the pot while the gear is deployed. This method nearly eliminates the line in the water column, which should also remove the risk of entanglement almost completely. Although this technique is widely considered the safest for whales and leatherback sea turtles prone to entanglement in fishing ropes, and the technology has existed for many years that can be used in pot fishing gear, considerable evaluation of this method is still needed that must especially address the relative cost, safety, reliability, and an alternative to buoys at the surface of the water that are used not only by their owners but also other fishermen and boaters that use them to avoid conflicts with the gear set below.

It is our intention that the VWES developed under this project will assist marine mammal scientists, fisheries experts, fishing gear designers, and bycatch reduction scientists in understanding what gear types and what whale behaviors lead to entanglements. In this vein, we hope to produce a more user-friendly version of the model that can be shared as a tool for evaluating the efficacy of different gear types and modifications. Additionally, through the virtual testing of different, perhaps new or untested gear types, the VWES will help to identify promising new gear techniques to help to avoid baleen whale entanglements and/or to lessen the severity of entanglements that do occur. While our focus was on the NARW, additional species that are prone to entanglements in buoy lines such as other baleen whales and leatherback sea turtles, could be examined using the model if adequate models are constructed and programmed with the correct articulations and swimming behaviors.

### ACKNOWLEDGMENTS

We would like to thank Drs. Anna E. Nousek-McGregor and Ross McGregor for providing the initial whale model. Portions of this investigation were supported by U.S. DOC-NOAA Grant# NA09NMF4520413 and NA10NMF4520343 to the Bycatch Consortium based at the New England Aquarium, U.S. DOC-NOAA Grant# NA13NMF4720280, and by nonfederal support to the New England Aquarium.

### LITERATURE CITED

Baldwin, K., T. Pickett, B. Brickett and S. Moffet. 2009. Assessing right whale entanglement risk through in situ, gear-whale flipper interaction experiments. New England Aquarium, Boston, MA.



- Barratclough, A., P. D. Jepson, P. K. Hamilton, C. A. Miller, K. Wilson and M. J. Moore. 2014. How much does a swimming, underweight, entangled right whale (*Eubalaena glacialis*) weigh? Calculating the weight at sea, to facilitate accurate dosing of sedatives to enable disentanglement. *Marine Mammal Science* 30:1589–1599.
- Brillant, S. W., and E. A. Trippel. 2010. Elevations of lobster fishery groundlines in relation to their potential to entangle endangered North Atlantic right whales in the Bay of Fundy, Canada. *ICES Journal of Marine Science* 67: 355–364.
- Budiman, J., S. Fuwa and K. Ebata. 2004. Fundamental studies on the hydrodynamic resistance of small pot traps. *Fisheries Science* 70:952–959.
- Cassoff, R. M., K. M. Moore, W. A. McLellan, S. G. Barco, D. S. Rotstein and M. J. Moore. 2011. Lethal entanglement in baleen whales. *Diseases of Aquatic Organisms* 96:175–185.
- Cawood, S., and P. McGee. 2009. Microsoft XNA Game Studio creator's guide. McGraw-Hill, New York, NY.
- Costello, G. A. 1997. *Theory of wire rope*. Springer, New York, NY.
- DigitalRune. 2014. DigitalRune Engine: 3D game engine for .NET and XNA. Available at <https://github.com/DigitalRune/DigitalRune>.
- Eloy, C. 2012. Optimal Strouhal number for swimming animals. *Journal of Fluids and Structures* 30:205–218.
- Emperore, K., and D. Sherry. 2015. *Unreal engine physics essentials*. Packt Publishing Ltd., Birmingham, U.K.
- Ericson, C. 2004. Real-time collision detection. in *The Morgan Kaufmann Series in Interactive 3D Technology*. CRC Press, Boca Raton, FL.
- Flory, J. F., C. M. Leech, S. J. Banfield and D. J. Petruska. 2005. Computer model to predict long-term performance of fiber rope mooring lines. *Offshore Technology Conference*, Houston, TX.
- Fridman, A. L. 2008. *Calculations for fishing gear designs*. Pierides Press, La Vergne, TN.
- Harbour, J. S. 2010. *The complete XNA 4.0*. Cengage Learning, Boston, MA.
- Harbour, J. S. 2012. *XNA Game Studio 4.0 for Xbox 360 developers*. Cengage Learning, Boston, MA.
- Imanishi, E., T. Nanjo and T. Kobayashi. 2009. Dynamic simulation of wire rope with contact. *Journal of Mechanical Science and Technology* 23:1083–1088.
- Imrak, C. E., and C. Erdonmez. 2010. On the problem of wire rope model generation with axial loading. *Mathematical and Computational Applications* 15:259–268.
- Iuppa, N. V., and T. Borst. 2010. *End-to-end game development: Creating independent serious games and simulations from start to finish*. Focal Press, Burlington, MA.
- Jaegers, K. 2010. *XNA 4.0 game development by example: Beginner's guide*. PACKT Publishing, Birmingham, U.K.
- Johnson, A., G. Salvador, J. Kenney, J. Robbins, S. Kraus, S. Landry and P. Clapham. 2005. Fishing gear involved on entanglements of right and humpback whales. *Marine Mammal Science* 21:635–645.
- Knowlton, A. R., P. K. Hamilton, M. K. Marx, H. M. Pettis and S. D. Kraus. 2012. Monitoring North Atlantic right whale *Eubalaena glacialis* entanglement rates: A 30 yr retrospective. *Marine Ecology Progress Series* 466:293–302.
- Kraus, S. D. C., and M. Hagbloom. 2016. *Project 4 Report: Assessments of vision to reduce right whale entanglements*. Consortium for Wildlife Bycatch Reduction. New England Aquarium, Boston, MA. 15 pp.
- Laist, D. W., A. R. Knowlton and D. Pendleton. 2014. Effectiveness of mandatory vessel speed limits for protecting North Atlantic right whales. *Endangered Species Research* 23:133–147.

- Lee, C. W., J. H. Lee, B. J. Cha, H. Y. Kim and J. H. Lee. 2005. Physical modeling for underwater flexible systems dynamic simulation. *Ocean Engineering* 32:331–347.
- Lever, N. 2001. Real-time 3D character animation with Visual C++. Focal Press, Waltham, MA.
- McCarron, P., and H. Tetreault. 2012. Lobster pot gear configurations in the Gulf of Maine. Consortium for Wildlife Bycatch Reduction, Maine Lobstermen's Association. New England Aquarium, Boston, MA. Page 36.
- McKenna, H. A., J. W. S. Hearle and N. O'Hear. 2004. Handbook of fibre rope technology. CRC Press, Boca Raton, FL.
- Miles, R. 2011. Microsoft XNA Game Studio 4.0: Earn programming now! Microsoft Press, Redmond, WA.
- Miller, T., and D. Johnson. 2011. XNA Game Studio 4.0 programming: Developing for Windows Phone 7 and Xbox. Addison Wesley, Upper Saddle River, NJ. Page 360.
- Miller, F. P., A. F. Vandome and J. McBrewster, eds. 2009. Comparison of OpenGL and Direct3D. Alphascript Publishing, Beau Bassin, Mauritius.
- Moore, M. J., and J. M. van der Hoop. 2012. The painful side of trap and fixed net fisheries: Chronic entanglement of large whales. *Journal of Marine Biology* 2012:Article ID 230653:4.
- Moore, M. J., A. Bogomolni, R. Bowman, *et al.* 2006. Fatally entangled right whales can die extremely slowly. Pages 675–677 *in* Oceans. IEEE, Boston, MA. Page 2006.
- Myers, R. A., S. A. Boudreau, R. D. Kenney, M. J. Moore, A. A. Rosenberg, S. A. Sherrill-Mix and B. Worm. 2007. Saving endangered whales at no cost. *Current Biology* 17:R10–R11.
- NOAA Fisheries. 2018. 2017–2018 North Atlantic right whale Unusual Mortality Event. Available at <https://www.fisheries.noaa.gov/national/marine-life-distress/2017-2018-north-atlantic-right-whale-unusual-mortality-event>.
- Nousek-McGregor, A. E. 2010. The cost of locomotion and North Atlantic right whales *Eubalaena glacialis*. Ph.D. thesis, Duke University, Durham, NC. 158 pp.
- Pace, R. M., T. V. N. Cole and A. G. Henry. 2014. Incremental fishing gear modifications fail to significantly reduce large whale serious injury rates. *Endangered Species Research* 26:115–126.
- Pace, R. M. III, P. J. Corkeron and S. D. Kraus. 2017. State-space mark-recapture estimates reveal a recent decline in abundance of North Atlantic right whales. *Ecology and Evolution* 7:8730–8741.
- Pettis, H. M., R. M. Rolland, P. K. Hamilton, S. Brault, A. R. Knowlton and S. D. Kraus. 2004. Visual health assessment of North Atlantic right whales (*Eubalaena glacialis*) using photographs. *Canadian Journal of Zoology* 82:8–19.
- Reed, A. 2011. Learning XNA 4.0. O'Reilly, Sebastopol, CA.
- Robbins, J., A. R. Knowlton and S. Landry. 2015. Apparent survival of North Atlantic right whales after entanglement in fishing gear. *Biological Conservation* 191:421–427.
- Rohr, J. J., and F. E. Fish. 2004. Strouhal numbers and optimization of swimming by odontocete cetaceans. *Journal of Experimental Biology* 207:1633–1642.
- Servin, M., C. Lacoursiere, F. Nordfelth and K. Bodin. 2011. Hybrid, multiresolution wires with massless frictional contacts. *IEEE Transactions on Visualization and Computer Graphics* 17:970–982.
- Tahar, A., and M. H. Kim. 2008. Coupled-dynamic analysis of floating structures with polyester mooring lines. *Ocean Engineering* 35:1676–1685.

- Taylor, G. K., R. L. Nudds and A. L. R. Thomas. 2003. Flying and swimming animals cruise at a Strouhal number tuned for high power efficiency. *Nature* 425:707–711.
- Tsukrov, I., O. Eroshkin, W. Paul and B. Celikkol. 2005. Numerical modeling of nonlinear elastic components of mooring systems. *IEEE Journal of Ocean Engineering* 30:37–46.
- U.S. Federal Register. 2013. Endangered Fish and Wildlife; Final Rule To Remove the Sunset Provision of the Final Rule Implementing Vessel Speed Restrictions To Reduce the Threat of Ship Collisions With North Atlantic Right Whales. FR 78(236):73726–73736 (9 December 2013). National Marine Fisheries Service, National Oceanic and Atmospheric Administration, Department of Commerce, Washington, DC.
- van der Hoop, J., M. Moore, A. Fahlman, *et al.* 2014. Behavioral impacts of disentanglement of right whale under sedation and the energetic cost of entanglement. *Marine Mammal Science* 30:282–307.
- van der Hoop, J. M., P. Corkeron, J. Kenny, S. Landry, D. Morin, J. Smith and M. J. Moore. 2016. Drag from fishing gear entangling North Atlantic right whales. *Marine Mammal Science* 32:619–642.
- van der Hoop, J. M., P. Corkeron, A. G. Henry and A. R. Knowlton. 2017. Predicting lethal entanglements as a consequence of drag from fishing gear. *Marine Pollution Bulletin* 115:91–104.

Received: 15 August 2017

Accepted: 31 August 2018

#### SUPPORTING INFORMATION

The following supporting information is available for this article online at <http://onlinelibrary.wiley.com/doi/10.1111/mms.12562/supinfo>.

*Figure S1.* Example gear configuration used for whale entanglement simulations. The trap (shown) is connected to a surface buoy (not shown) by a bridle, gangion line, a section of floating line, and a section of sinking line.